Interference-enhanced infrared-to-visible upconversion in solid-state thin films sensitized by colloidal nanocrystals

Mengfei Wu, Joel Jean, Vladimir Bulović, and Marc A. Baldo

Citation: Appl. Phys. Lett. **110**, 211101 (2017); doi: 10.1063/1.4984136
View online: http://dx.doi.org/10.1063/1.4984136
View Table of Contents: http://aip.scitation.org/toc/apl/110/21
Published by the American Institute of Physics

Interference-enhanced infrared-to-visible upconversion in solid-state thin films sensitized by colloidal nanocrystals

Mengfei Wu, Joel Jean, Vladimir Bulović, and Marc A. Baldo[a)]
Energy Frontier Research Center for Excitonics, Massachusetts Institute of Technology, Cambridge, Massachusetts 02139, USA

(Received 17 March 2017; accepted 12 May 2017; published online 22 May 2017)

Infrared-to-visible photon upconversion has potential applications in photovoltaics, sensing, and bioimaging. We demonstrate a solid-state thin-film device that utilizes sensitized triplet-triplet exciton annihilation, converting infrared photons absorbed by colloidal lead sulfide nanocrystals (NCs) into visible photons emitted from a luminescent dopant in rubrene at low incident light intensities. A typical bilayer device consisting of a monolayer of NCs and a doped film of rubrene is limited by low infrared absorption in the thin NC film. Here, we augment the bilayer with an optical spacer layer and a silver-film back reflector, resulting in interference effects that enhance the optical field and thus the absorption in the NC film. The interference-enhanced device shows an order-of-magnitude increase in the upconverted emission at the wavelength of $\lambda = 610$ nm when excited at $\lambda = 980$ nm. At incident light intensities above 1.1 W/cm^2, the device attains maximum efficiency, converting $(1.6 \pm 0.2)\%$ of absorbed infrared photons into higher-energy singlet excitons in rubrene. *Published by AIP Publishing.* [http://dx.doi.org/10.1063/1.4984136]

Infrared-to-visible upconversion devices turn two or more low-energy infrared photons into a higher-energy visible photon. Such devices could extend the fraction of the solar spectrum usable by a solar cell,[1] expand the material choices for infrared detection and imaging, and aid in deep-tissue bioimaging.[2] Notably, infrared-to-visible upconversion can sensitize silicon to sub-bandgap light, which could lead to enhanced solar cell performance and relatively inexpensive infrared imaging arrays. A typical approach to converting infrared into visible light uses lanthanide ions doped in a bulk[3] or nanoparticle[2] host matrix, exploiting their multiple ladder-like and long-lived excited states.[4] The lanthanides, however, have narrow and relatively weak absorption,[4] necessitating high excitation intensity on the order of 100 W/cm^2 to attain efficient upconversion.[5,6] Recently, infrared-to-visible upconversion based on triplet-triplet exciton annihilation (TTA)[7,8] sensitized by colloidal nanocrystals (NCs) has been reported in both solutions[9] and solid-state films.[10] Importantly, the long lifetime of molecular triplets[11] and the relatively strong and broadband absorption of the NC sensitizer[12] allow for upconversion even when the incident light is incoherent and of low intensity. TTA-based upconversion reaching an efficiency of $(8.4 \pm 1.0)\%$ with pump wavelength $\lambda = 808$ nm and incident light intensity as low as 3.2 mW/cm^2 has been demonstrated in solutions.[13] In the solid state, however, state-of-the-art devices require 12 W/cm^2 of incident light at $\lambda = 808$ nm.[10] Here, we report an interference-enhanced thin-film upconversion device that operates efficiently with an excitation intensity of 1.1 W/cm^2, pumped at $\lambda = 980$ nm.

Our previous work demonstrates a solid-state device that upconverts from $\lambda > 1\ \mu$m to $\lambda = 610$ nm.[10] The device consists of a spin-cast monolayer of colloidal lead sulfide (PbS) NCs capped with oleic acid ligands and an 80 nm-thick thermally evaporated film of rubrene doped with 0.5 vol. % of dibenzotetraphenylperiflanthene (DBP); see Fig. 1(a). As depicted in Fig. 1(b), the NC quantum dots absorb incident infrared photons and form excitons, which transfer energy to rubrene molecules, promoting them to excited spin-triplet states. When two rubrene triplets meet, they can undergo TTA to form a higher-energy spin-singlet exciton, which then transfers energy to the dopant DBP. Excited DBP molecules relax to give visible light.

One key limitation in the bilayer solid-state device is that the NC film has to be kept as thin as one or two monolayers to maximize the upconverted emission.[10] This is likely due to short exciton diffusion length in PbS NCs capped with long oleic acid ligands,[14] as well as increased re-absorption of visible emission in thicker NC films. As a result, the thin NC film in the device absorbs less than 0.5% of incident infrared light.

In the present study, we improve the bilayer device by adopting a device structure similar to a critically coupled resonator,[15] in which interference effects lead to increased infrared absorption in the NC film. On top of the original bilayer, we deposit a thin layer of tris-(8-hydroxyquinoline)aluminum (AlQ_3) and a 100 nm-thick film of silver by thermal evaporation; see Fig. 1(c). Glass substrates are cleaned by sequential sonication in 2% detergent solution, deionized water, and acetone, followed by immersion in boiling isopropanol. The NC film and the subsequent layers appear uniform and smooth to the naked eye, although under an atomic force microscope, the NC film has sites which are a monolayer higher or lower than the average.[10] In addition, crystallites tend to form in the rubrene film after a few days. The devices are encapsulated in a nitrogen atmosphere with two-part epoxy and a piece of cover glass and are characterized under ambient conditions within 24 h.

The AlQ_3 film with a wide bandgap of (2.7 ± 0.1) eV[16] does not absorb the incident light but acts as an optical spacer layer, separating the reflective silver interface from the optically active layers. The presence of a back reflector, together

a)Electronic mail: baldo@mit.edu

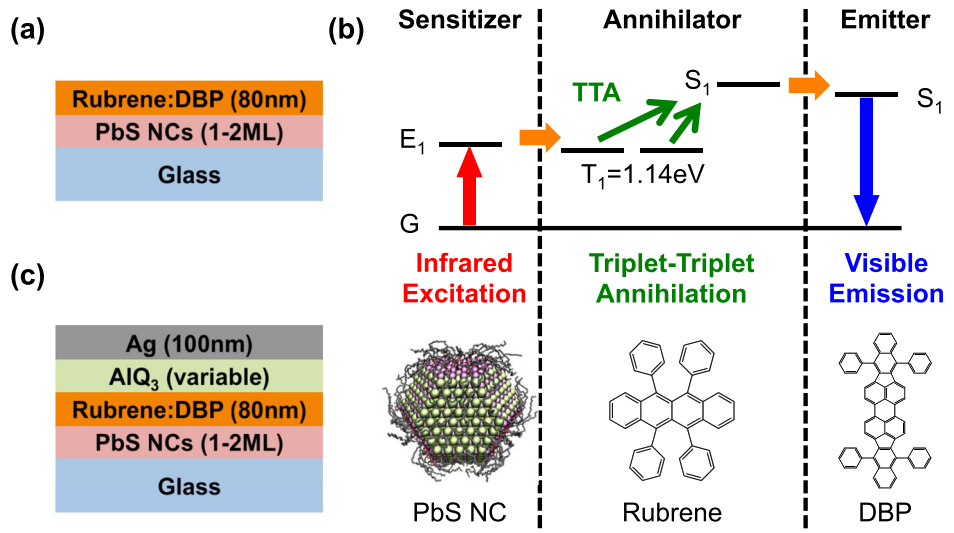

FIG. 1. (a) Solid-state device structure for upconversion consisting of 1–2 monolayers (ML) of PbS nanocrystals (NCs) capped with oleic acid ligands and 80 nm-thick rubrene doped with 0.5 vol. % of DBP. (b) Schematic illustration of upconversion via triplet-triplet annihilation (TTA) sensitized by colloidal PbS NCs. The process involves absorption of incident infrared light in the NCs, triplet energy transfer to rubrene, TTA in rubrene, singlet energy transfer to DBP, and emission of visible light from DBP. (c) Interference-enhanced device structure for upconversion. An AlQ_3 optical spacer layer and 100 nm-thick silver rear reflector are added to increase infrared absorption in the NC film.

with the small layer thicknesses compared to the coherence length of the incident light, results in interference between the incident and reflected waves. By tuning the thickness of the AlQ_3 layer, one can maximize the optical field at the position of the active NC film, thereby enhancing absorption of the incident infrared light. In this work, we use PbS NC thin films with the lowest-energy exciton absorption peak at $\lambda = 960$ nm. The device exhibits upconverted photoluminescence (PL) at $\lambda = 610$ nm when pumped at $\lambda = 980$ nm, as shown in Fig. 2.

The light absorption in our device structures can be modeled using the transfer matrix method, as has previously been done for 1-D light propagation and absorption in organic thin-film solar cells with reflective electrodes.[17,18] In the model, we assume that the device consists of a 10 nm-thick layer (~2 monolayers) of $\lambda = 960$ nm PbS NCs on glass, 80 nm-thick rubrene, varying thicknesses of the AlQ_3 layer, and 100 nm of silver. By adjusting the AlQ_3 layer thickness, we can maximize the optical field intensity at the

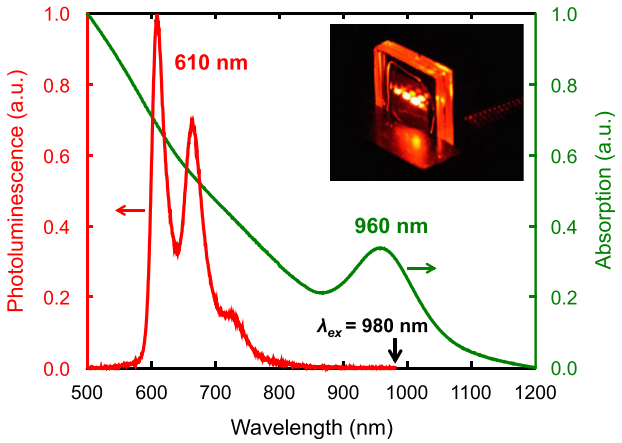

FIG. 2. Absorption spectrum of a thin film of $\lambda = 960$ nm PbS nanocrystals (NCs) and upconverted emission from DBP when the NC-sensitized device is excited at $\lambda = 980$ nm. Inset: photograph of an upconverting device glowing under $\lambda = 980$ nm pump light incident at a shallow angle.

NC layer, therefore enhancing the infrared absorption. The optical constants used in the model are obtained by spectroscopic ellipsometry on individual films. With excitation at $\lambda = 980$ nm and at normal incidence, the optical electric field intensity at the NC layer is computed to be maximized with 20 nm-thick AlQ_3; see Fig. 3(a). Compared to the bilayer-only device, the optimized device structure should increase the absorption in the NC film by over five times.

Experimentally, we measure the upconverted PL of interference-enhanced devices sensitized by $\lambda = 960$ nm NCs and excited at $\lambda = 980$ nm; see Fig. 3(b). The PL is collected from the same side as the incident beam. The results show a slight deviation from our absorption model: visible emission is maximized when the AlQ_3 spacer layer is 30 nm thick instead of 20 nm. The optimized device enhances the upconverted PL integrated from $\lambda = 550$ nm to $\lambda = 850$ nm by about 11 times, approximately twice the calculated enhancement in absorption alone; see Fig. 3(a). The factor of two is partly due to the redirection of the upconverted light that would otherwise have exited from the back of the device toward the front face by the silver mirror. In addition to the slight shift in the optimal spacer thickness, the dependence of the observed visible emission on the spacer thickness is more pronounced than that of the modeled absorption and varies with the emission wavelength, as seen in Fig. 3(b). These differences can be attributed to changes in the emission pattern and outcoupling efficiency of the visible light in the rubrene:DBP layer in the presence of a rear silver reflector.[19,20]

We then measure the dependence of upconverted PL on incident light intensity. As shown in Fig. 4, the interference-enhanced device structure increases the PL integrated from $\lambda = 550$ nm to $\lambda = 850$ nm by an order of magnitude over a range of incident intensities. Typical for TTA-based upconversion,[21] at relatively weak excitation, the upconverted PL depends quadratically on the incident intensity, when most of the triplets do not undergo TTA upconversion, but are lost via

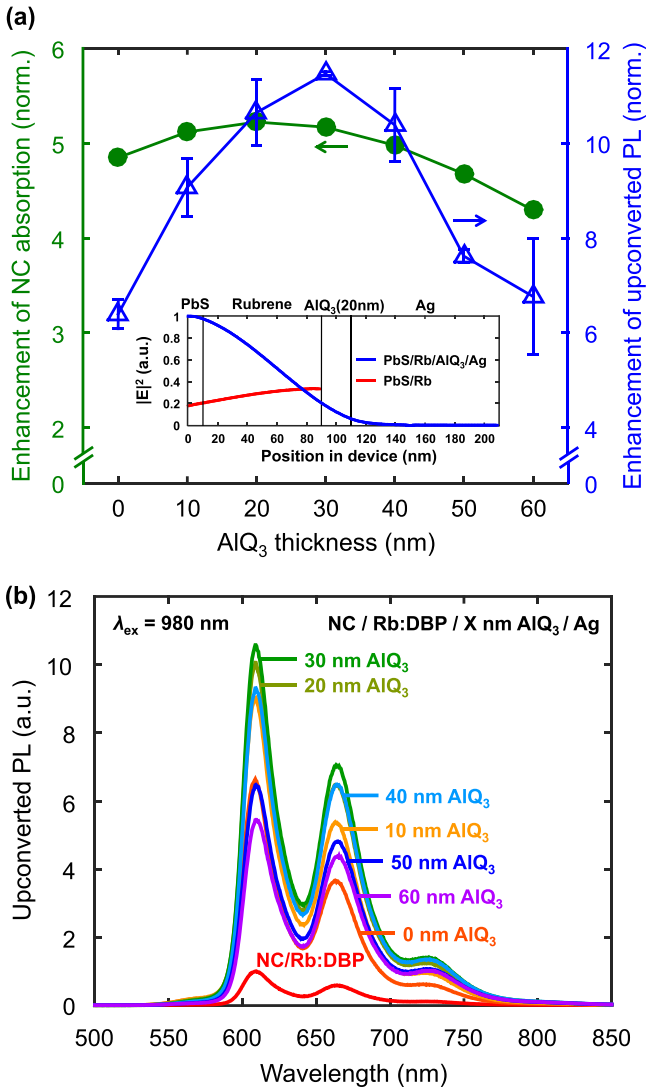

FIG. 3. Devices with varying thicknesses of the AlQ_3 spacer layer, capped with a 100 nm-thick silver film. (a) Left y-axis: enhancement of nanocrystal (NC) absorption at $\lambda = 980$ nm, normalized to a bilayer device, modeled by the transfer matrix method at normal incidence. Inset: simulated electric field intensity profile in a bilayer device and in a device with 20 nm of AlQ_3. Right y-axis: enhancement of upconverted PL, measured for devices sensitized by $\lambda = 960$ nm NCs pumped at $\lambda = 980$ nm. The enhancement is calculated by integrating each PL spectrum in (b) from $\lambda = 550$ nm to $\lambda = 850$ nm, and normalizing it to the PL of a bilayer device. Experimentally, upconverted emission is maximized with 30 nm of AlQ_3 and is about 11 times higher than that in a bilayer device.

first-order processes such as conventional non-radiative decay. The dependence switches to linear at higher incident intensities, when the triplet density becomes sufficiently high for bimolecular TTA to dominate, leading to maximum upconversion yield. In other words, the quantum yield increases linearly at low intensities and plateaus to a maximum value at high intensities. The intensity at which the upconverted PL becomes linear, and the yield approaches the maximum, is termed the threshold intensity. It indicates the minimum incident intensity required to attain efficient upconversion. Enhanced by interference effects, the device with 20 nm-thick AlQ_3 and a silver back reflector displays a threshold intensity of 1.1 W/cm^2 when excited at $\lambda = 980$ nm, one-third of that required for the original bilayer device and two orders of magnitude lower than typical lanthanide-based upconverters.[5,6]

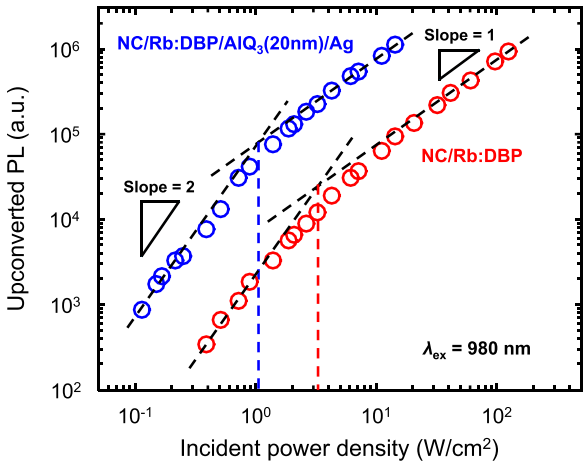

FIG. 4. Dependence of upconverted PL integrated from $\lambda = 550$ nm to $\lambda = 850$ nm on incident light intensity for devices sensitized by $\lambda = 960$ nm nanocrystals (NC) excited at $\lambda = 980$ nm. An interference-enhanced device (blue) is an order of magnitude brighter than a bilayer device (red) at each incident power density. The threshold intensity, where the PL dependence transitions from quadratic to linear, is reduced from 3.3 W/cm^2 in the bilayer to 1.1 W/cm^2 in the enhanced device.

To determine the upconversion efficiency, we measure the absorption and visible PL of the optimized device in an integrating sphere at two excitation wavelengths: $\lambda = 980$ nm and $\lambda = 450$ nm. We define the upconversion efficiency (η_{UC}) as the fraction of absorbed infrared photons that turn into higher-energy singlets in rubrene. This is equivalent to the PL quantum yield of infrared-to-visible upconversion divided by the PL quantum yield of doped rubrene and multiplied by two to normalize the maximum upconversion quantum efficiency.[2,7] This definition of η_{UC} allows us to probe the combined efficiency of triplet energy transfer and TTA, isolated from the emission efficiency of the rubrene layer, which varies with thickness and dopant concentration. Experimentally, η_{UC} can be determined by

$$\eta_{UC} = \frac{P_{\lambda=980nm}}{L_{\lambda=980nm} \cdot A_{\lambda=980nm}} \cdot \frac{L_{\lambda=450nm} \cdot A_{\lambda=450nm}}{P_{\lambda=450nm}} \cdot 2 \cdot 100\%.$$

The subscripts indicate the pump wavelength. P is the visible PL intensity measured by a lock-in photodetector at the exit port of the integrating sphere. L is the number of photons in the incident laser beam, measured by a calibrated power meter. A is the absorption in the active material, i.e., NCs at $\lambda = 980$ nm and doped rubrene at $\lambda = 450$ nm. Absorption is measured by comparing the difference in laser intensity exiting the sphere with and without the sample inside. Parasitic absorption in the silver layer is accounted for by subtracting the absorption of a control sample consisting of glass/AlQ_3/silver/glass. For an interference-enhanced device with a monolayer of $\lambda = 960$ nm NCs and 80 nm-thick doped rubrene, absorption in the PbS NC film at pump wavelength $\lambda = 980$ nm is $(1.5 \pm 0.2)\%$, and absorption in the rubrene film at pump wavelength $\lambda = 450$ nm is $(20 \pm 1)\%$. By comparing the absorption and PL signals at the two excitation wavelengths, we measure an upconversion efficiency of $(1.6 \pm 0.2)\%$.

In the absence of a silver reflector, the upconversion efficiency of a bilayer device sensitized by $\lambda = 960$ nm NCs

is $\eta_{UC} = (0.51 \pm 0.07)\%$ when excited at $\lambda = 808\,\text{nm}$.[10] The lower efficiency is partly due to the difference in the emission pattern with a smaller fraction of upconverted light scattered out of the sample when the silver mirror is absent.[19] But we also expect that efficiency measurements in the interference-enhanced structure are less subject to parasitic losses. The single-pass absorption of a monolayer NC film in a bilayer device is too low to be measured reliably with the usual angle of incidence ($\sim 35^\circ$ with respect to the normal) given the noise floor of our integrating sphere setup. To boost the infrared absorption, a device can be pumped at a shallow angle with the laser beam landing at the edge of the glass substrate and traversing the entire sample length,[10] increasing the effective path length of light. However, in such an edge-pumped geometry, the measured absorption includes parasitic losses such as scattering by the epoxy and reflection by the edge of the glass substrate out of the sphere. The value of η_{UC} reported previously[10] is thus a lower bound of the upconversion efficiency. Here, the devices with interference enhancement have increased absorption that can be measured reliably with the conventional incident angle, which minimizes parasitic losses by confining as much light as possible within the sphere. The interference-enhanced device structure therefore enables more accurate determination of η_{UC}.

In summary, we present a simple, improved device structure for solid-state infrared-to-visible upconversion sensitized by colloidal NCs. We incorporate an optical spacer and a silver reflector to optimize interference effects and achieve improved infrared absorption, enhanced upconverted PL, and reduced threshold intensity. More sophisticated reflective structures, such as distributed Bragg reflectors,[15] can potentially be used to further boost infrared absorption and visible emission. This work highlights the benefits of optical management in solid-state upconverting devices and brings NC-sensitized infrared-to-visible upconversion a step closer to integration for photovoltaic, sensing, and imaging applications.

This work was supported as part of the Center for Excitonics, an Energy Frontier Research Center funded by the U.S. Department of Energy, Office of Science, Office of Basic Energy Sciences under Award No. DE-SC0001088 (MIT). The authors would like to thank Professor Moungi Bawendi's group for providing synthesized nanocrystals. M.W. acknowledges insightful discussions with Farnaz Niroui and Thomas Mahony.

[1]T. Trupke, A. Shalav, B. S. Richards, P. Würfel, and M. A. Green, Sol. Energy Mater. Sol. Cells **90**, 3327 (2006).
[2]J. Zhou, Q. Liu, W. Feng, Y. Sun, and F. Li, Chem. Rev. **115**, 395 (2015).
[3]F. Auzel, Chem. Rev. **104**, 139 (2004).
[4]J.-C. G. Bünzli and C. Piguet, Chem. Soc. Rev. **34**, 1048 (2005).
[5]R. H. Page, K. I. Schaffers, P. A. Waide, J. B. Tassano, S. A. Payne, W. F. Krupke, and W. K. Bischel, J. Opt. Soc. Am. B **15**, 996 (1998).
[6]J.-C. Boyer and F. C. J. M. van Veggel, Nanoscale **2**, 1417 (2010).
[7]T. N. Singh-Rachford and F. N. Castellano, Coord. Chem. Rev. **254**, 2560 (2010).
[8]T. F. Schulze and T. W. Schmidt, Energy Environ. Sci. **8**, 103 (2015).
[9]Z. Huang, X. Li, M. Mahboub, K. M. Hanson, V. M. Nichols, H. Le, M. L. Tang, and C. J. Bardeen, Nano Lett. **15**, 5552 (2015).
[10]M. Wu, D. N. Congreve, M. W. B. Wilson, J. Jean, N. Geva, M. Welborn, T. Van Voorhis, V. Bulović, M. G. Bawendi, and M. A. Baldo, Nat. Photonics **10**, 31 (2016).
[11]S. Reineke and M. A. Baldo, Sci. Rep. **4**, 3797 (2014).
[12]I. Moreels, K. Lambert, D. Smeets, D. De Muynck, T. Nollet, J. C. Martins, F. Vanhaecke, A. Vantomme, C. Delerue, G. Allan, and Z. Hens, ACS Nano **3**, 3023 (2009).
[13]M. Mahboub, Z. Huang, and M. L. Tang, Nano Lett. **16**, 7169 (2016).
[14]G. M. Akselrod, F. Prins, L. V. Poulikakos, E. M. Y. Lee, M. C. Weidman, A. J. Mork, A. P. Willard, V. Bulović, and W. A. Tisdale, Nano Lett. **14**, 3556 (2014).
[15]J. R. Tischler, M. S. Bradley, and V. Bulović, Opt. Lett. **31**, 2045 (2006).
[16]P. E. Burrows, Z. Shen, V. Bulović, D. M. McCarty, S. R. Forrest, J. A. Cronin, and M. E. Thompson, J. Appl. Phys. **79**, 7991 (1996).
[17]L. A. A. Pettersson, L. S. Roman, and O. Inganäs, J. Appl. Phys. **86**, 487 (1999).
[18]P. Peumans, A. Yakimov, and S. R. Forrest, J. Appl. Phys. **93**, 3693 (2003).
[19]R. R. Chance, A. Prock, and R. Silbey, in *Advances in Chemical Physics*, edited by I. Prigogine and S. A. Rice (Wiley, 1978), pp. 1–65.
[20]V. Bulović, V. B. Khalfin, G. Gu, P. E. Burrows, D. Z. Garbuzov, and S. Forrest, Phys. Rev. B **58**, 3730 (1998).
[21]A. Haefele, J. Blumhoff, R. S. Khnayzer, and F. N. Castellano, J. Phys. Chem. Lett. **3**, 299 (2012).